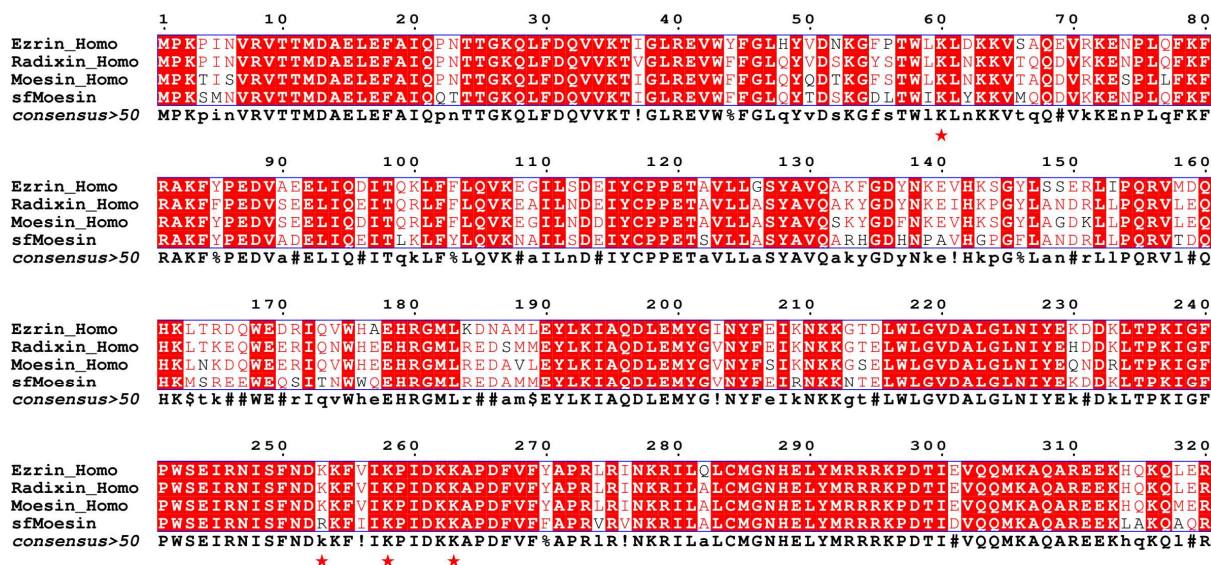


Figure S1

A



B

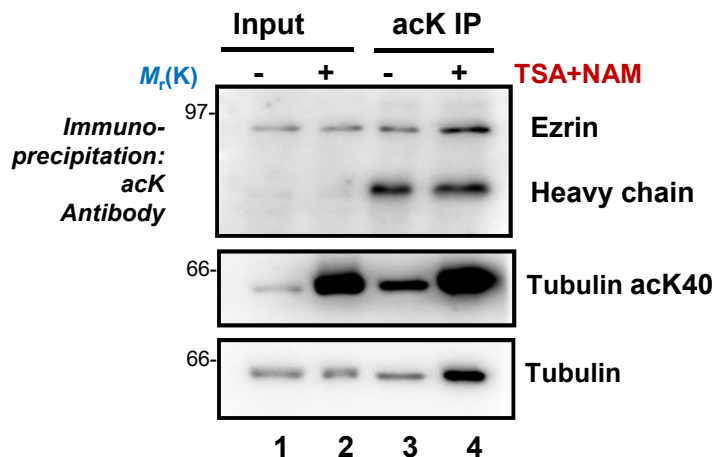
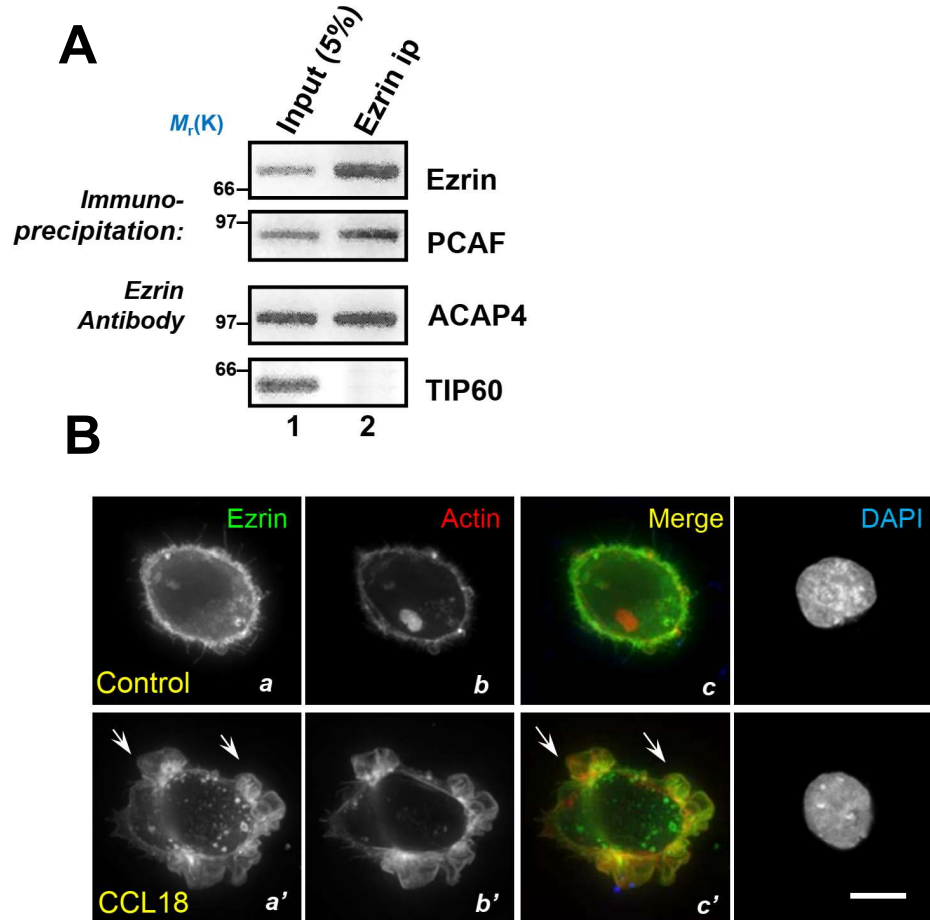


Figure S1. Ezrin acetylation sites are evolutionarily conserved

A. Sequence alignment of human ERM proteins and *Spodoptera frugiperda* Moesin. Ezrin (protein ID: P15311), Radixin (protein ID: P35241), Moesin (protein ID: P26038) and *Spodoptera frugiperda* Moesin (protein ID: A0T1L9). The four conserved acetylation sites (K60, K253, K258 and K263) are marked by red stars.

B. MDA-MB-231 cells were treated with DMSO or deacetylases inhibitors (1 μ M Trichostatin A (TSA) and 10 mM Nicotinamide (NAM)) for 4 h. The whole cell lysates were immunoprecipitated by anti-acetyllysine Agarose. Acetylated ezrin was detected by immunoblotting with ezrin antibody.

Figure S2



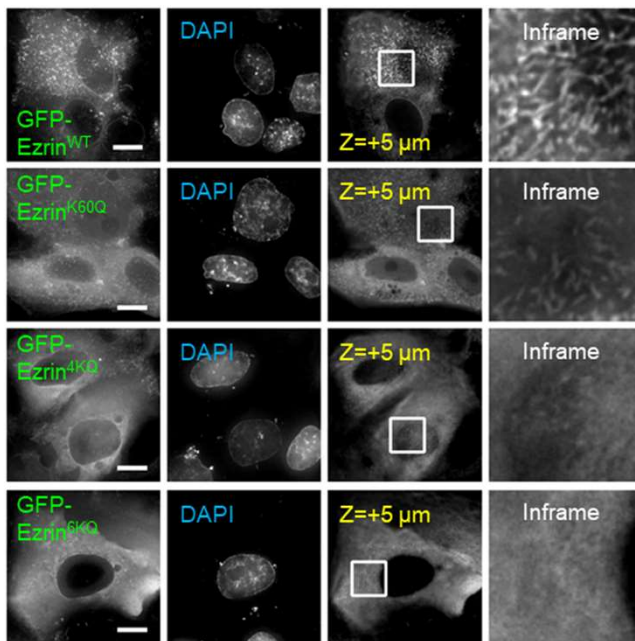
Figures S2. Ezrin-PCAF interactions in MDA-MB-468 cells

A. Western blotting analyses of ezrin-PCAF interaction in an anti-ezrin antibody immunoprecipitation of MDA-MB-468 cell lysates. Note that TIP60 is not recovered in anti-ezrin immunoprecipitates.

B. Actin and ezrin distribution profiles in the MDA-MB-468 cells. Cells were treated, fixed, permeabilized, and stained for endogenous ezrin (green), actin (red) and DAPI (blue). Bar, 10 μ m.

Figure S3

A



B

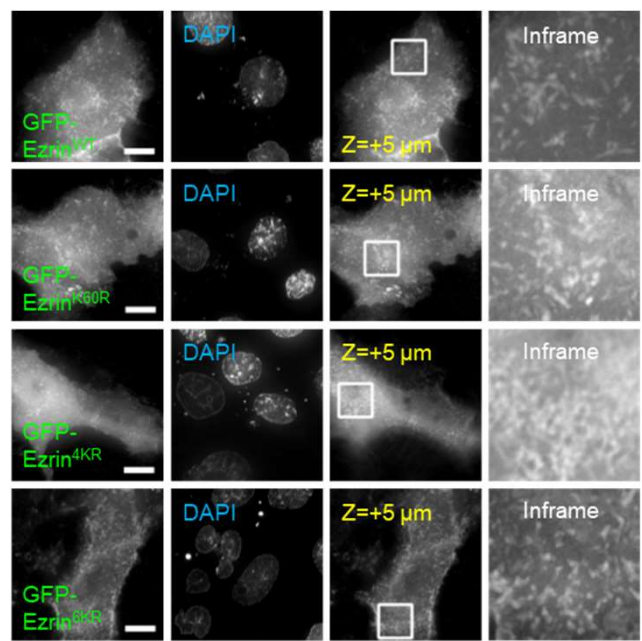


Figure S3. Acetylation of Ezrin abolishes its membrane or microvilli localization in LLC-PK1 cells

A. LLC-PK1 cells were transfected with GFP-Ezrin wild type and acetylation-mimicking mutants. To investigate the localization of Ezrin mutants in plasma membrane or microvilli, the Z stack picture, Z=5 μm, and in frame pictures were shown, respectively. Note that the membrane and microvilli localization of Ezrin^{4KQ} and Ezrin^{6KQ} were significantly diminished compared with Ezrin^{WT}. 4K represents K60, K253, K258 and K263 sites, and 6K represents K35, K60, K139, K253, K258 and K263 sites in Ezrin. Bar, 10 μm.

B. LLC-PK1 cells were transfected with non-acetylatable Ezrin mutants. To investigate the localization of non-acetylatable Ezrin in plasma membrane or microvilli, the Z stack picture, Z=5 μm, and in frame pictures were shown, respectively. Note that non-acetylatable Ezrin mutants localize at membrane or microvilli localization as wild type. Bar, 10 μm.

Figure S4

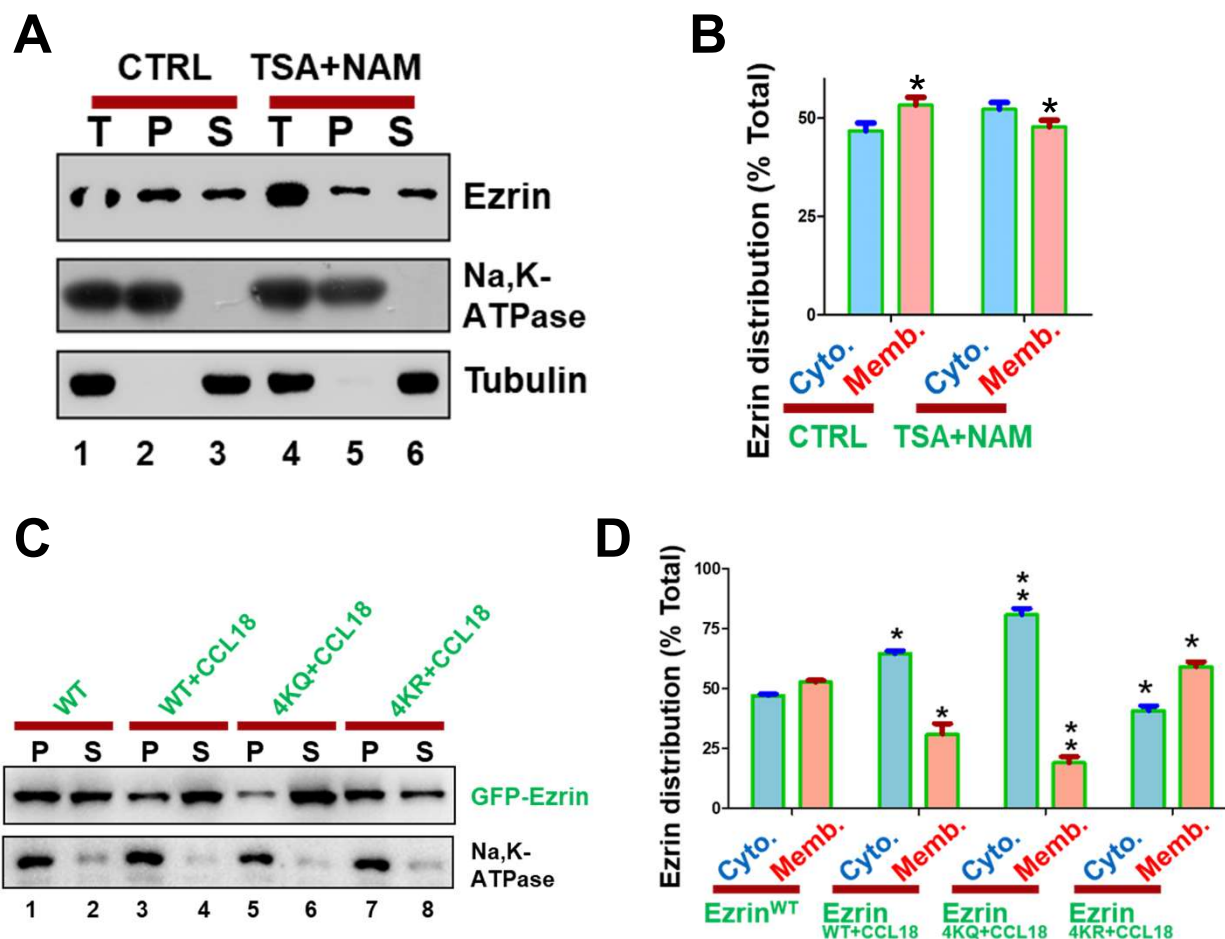


Figure S4. Ezrin translocates from membrane to cytosol *in vivo* upon acetylation

A. HEK293T cells were treated with DMSO or TSA and NAM for 4 h, and then cell fractionation was applied by velocity gradient centrifugation. Cell lysate input (T), suspension (S), and pellet (P) were analyzed by Western Blot. The plasma membrane fraction and cytoplasm fraction were indicated by Na, K-ATPase and tubulin blots, respectively.

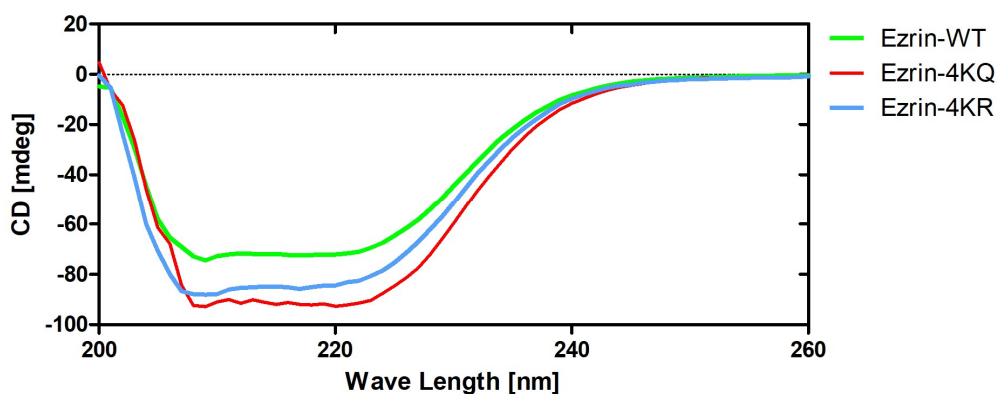
B. Quantitative analysis of cell fractionation assay in **A**. Data represents mean \pm SE from three independent experiments. * $P < 0.05$.

C. MBA-MD-231 cells were transfected with GFP-ezrin wild type and mutants, then cells were treated with CCL18 or not before cell fractionation assay. Suspension (S), and pellet (P) were analyzed by Western Blot. The plasma membrane fraction was indicated by Na, K-ATPase, respectively.

D. Quantitative analysis of cell fractionation assay in **C**. Data represents mean \pm SE from three independent experiments. *** $P < 0.001$, and * $P < 0.05$.

Figure S5

A



B

	Ezrin-WT	Ezrin-4KQ	Ezrin-4KR
α -Helix/%	27.3	32.7	25.8
β -Sheet/%	18.2	10.7	22.5
Turns/%	20.5	22.6	18.8
Random Coils/%	33.9	34	32.9
RMS*	3.359	4.793	3.657

CD spectra of Ezrin WT, Ezrin 4KR and Ezrin 4KQ using the Jasco Secondary Structure Estimation software by the reference CD (Yang-U).

*RMS<20 represent the above data is credible.

Figure S5. Ezrin exhibits a conformational change upon acetylation

A. Purified His-Ezrin WT and mutant proteins were analyzed by the spectropolarimeter. CD spectra were recorded in PBS at room temperature in a wavelength range of 260–200 nm with 1.0 nm bandwidth, using the continuous-mode setting, with 1.0 s response and a scan speed of 50 nm/min. Three spectra were averaged, spectra were background-corrected against pure buffer. For normalization, the final protein concentrations were determined by UV/Vis-spectroscopy using pure buffer for background correction. Deconvolution of the data was performed using the Jasco Secondary Structure Estimation software by the reference CD (Yang-U).

B. CD spectra of Ezrin WT, Ezrin 4KR and Ezrin 4KQ using the Jasco Secondary Structure Estimation software by the reference CD (Yang-U). *RMS<20 represent the above data is credible.

Figure S6

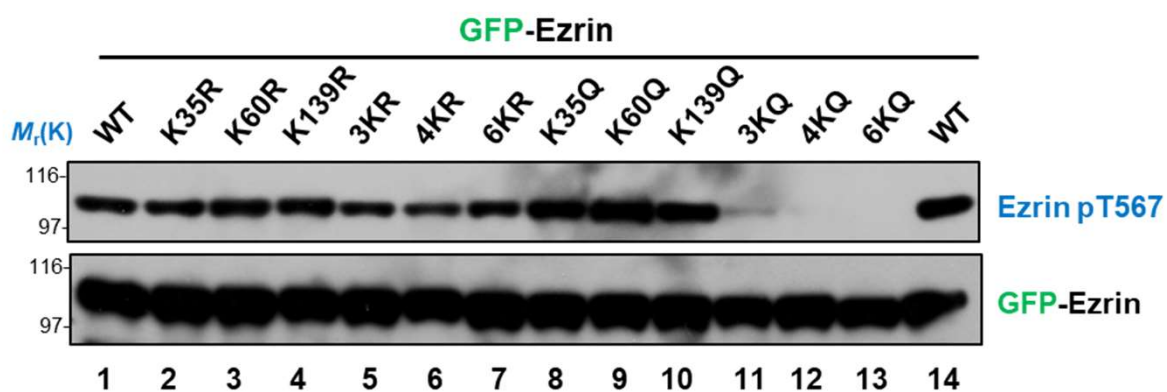


Figure S6. Ezrin acetylation prevents Ezrin T567 phosphorylation

HEK293T cells were transfected with GFP-Ezrin acetylation mutants. Whole cell lysates were separated by SDS-PAGE and blotted with indicated antibodies.